Paper technology

Marjo Järvinen, Riku Pihko and Jukka A. Ketoja*

Density development in foam forming: wet pressing dynamics

https://doi.org/10.1515/npprj-2018-3031
Received November 13, 2017; accepted February 14, 2018

Abstract: The compression behaviour of both foam and water formed wet sheets was studied in the laboratory. The development of sheet thickness was followed for different pressing dynamics including both short and long pulses. The immediate recovery of sheet thickness after the first short pressing pulse was clearly better for foam than for water. The bulk advantage of foam forming gradually reduced as the number of pressing pulses increased. The solids content after wet pressing became higher for foam than water forming. The differences in sheet density and dewatering for the two forming methods should be taken into account when developing industrial processes for lightweight fibre-based products.

Keywords: compression; density; foam; forming; solids content; water; wet pressing.

Introduction

Foam technology can lead to a leap in manufacturing of various fibre-based products including paper, board and packaging materials, nonwovens, filtering and construction materials (Radvan and Gatward 1972, Lehmonen et al. 2013, Poranen et al. 2013). Foam forming offers the possibility to form lightweight materials with tailored pore structures and density gradients near surfaces (Al-Qararah et al. 2015, Pöhler et al. 2016). However, the structure consolidation mechanisms in various process phases and their effect on the final product structure has not been fully understood. The difference in material density for foam and water forming is often thought to originate in the forming stage. Subsequent wet pressing, calendering and other compressive production operations are then expected to partly deteriorate the higher bulk obtained with foam forming. This conjecture has not been tested systematically before. For water forming, the effect of pressing on web properties has been studied in many previous works (Pikulik et al. 1998, Vomhoff 1998, van Lieshout 2006, Hii et al. 2012), but similar information for foam forming has been lacking.

The goal of the current work was to determine how water and foam formed webs differentiate during the wet pressing stage in respect to their compression behaviour. In particular, web thickness (bulk) and solids content development during forming and subsequent pressing was followed for different pressing pulses applied to wet laboratory sheets. The results suggest that web density can be controlled not only with the forming method but also with the wet pressing strategy.

***Corresponding author: Jukka A. Ketoja,** VTT Technical Research Centre of Finland Ltd, P. O. Box 1603, FI-40400, Jyväskylä, Finland, e-mail: jukka.ketoja@vtt.fi
Marjo Järvinen, Riku Pihko, VTT Technical Research Centre of Finland Ltd, P. O. Box 1603, FI-40400, Jyväskylä, Finland, e-mails: marjo.jarvinen@vtt.fi, riku.pihko@vtt.fi

Materials and methods

Pulp preparation

The study was based on a model furnish based on refined chemithermo-mechanical (CTMP) spruce pulp. Before sheet making, refined CTMP was disintegrated with hot tap water (temperature 55 °C) by using a pilot pulper. The disintegrated pulp was then fractionated to a long fibre fraction by using the Bauer McNett device. The device included two wide-mesh screens with sizes of 16 and 30 mesh/inch (approximately 1.19 mm and 0.595 mm, respectively). Fibres collected in the screens were used to make sheets. L&W FiberMaster was used for the analysis of fibre dimensions. The average length-weighted fibre length of the refined CTMP was 1.42 mm (freeness 53 ml) and after fractionation, the collected long-fibre fraction had an average length of 2.15 mm. The L&W fines content was 46 % for the initial refined CTMP and 5.5 % after the fractionation. In other words, the fractionated model furnish consisted mainly of long fibres, but there was a small amount of fines in the furnish as well.

Chemicals

Sodium dodecyl sulphate (SDS, Sigma-Aldrich) was used as a foaming aid in making the foam sheets. SDS is an anionic surfactant. The purity of SDS was 90 %. The purity refers to chain-length differences of surfactant components. Commercial SDS products are C12–C16 mixtures with C12 alkyl sulfate (dodecyl) component dominating. This is due to the fatty acid composition of the raw material (such as coconut oil) used in SDS manufacture.

SDS was delivered in a powdery form, and it was dissolved in deionized water before use: 100 g of SDS was added into a 1 liter volumetric flask and filled with deionized water to get 10 % stock solution. 12 ml of stock solution (containing 1.2 g of SDS) was added into the pulp (volume 2 l). Therefore the surfactant concentration was 0.6 g/l when making the fibre-foam suspensions.

Preparation of foam-formed sheets

Sheets of the size 35 cm × 22 cm with target grammage of 200 g/m^2 were made with a foam forming handsheet mould. The fibres were diluted with tap water to a consistency of 0.7 %. 2 l of this pulp was taken into a vessel (Ø 160 mm). The vessel was placed under the Netzsch ShearMaster mixer and clamped in. A mixing plate (Ø 83 mm) was placed a few millimetres below the surface of the pulp. The mixing plate was a circular disk, which had two opposing 25° bends with their fulcrum positioned at a distance of 0.32D from the centre of the plate (D being the diameter of the plate). Surfactant was added to pulp and the mixer was rotated at 3800 rpm to generate the foam. The mixer was stopped when the air content of the fibre-foam suspension was approximately 68 % (volume 6.3 l).

The fibre-foam suspension was poured into a funnel, which stood on the top of the mould. The funnel directed the fibre-foam to one side of the mould so that the suspension spread out evenly on top of the forming fabric. The funnel was then removed, and a plastic cover was placed on top of the fibre-foam to create a vacuum seal. The foam was sucked out through the fabric, after which the plastic cover was removed from sheet. The maximum vacuum level was ca. 0.5 bar, but this level was not constant during the consolidation phase (lasting around 10 s).

The wet sheet and the forming fabric were removed from the mould and the sheet, covered with two blotter papers, was couched by first placing a plastic plate on the top of the pile. The couching was done carefully by hand so that the plastic plate was pressed only slightly. After couching, the forming fabric and blotter papers were removed, and the wet sheet was stored between thin plastic sheets.

Preparation of water-formed sheets

The water-formed sheets were made with the same foam forming handsheet mould to ensure similar handling of sheets as in the case of foam forming. The target grammage was the same as for the foam-formed sheets, 200 g/m^2.

Fibres were diluted with tap water to a consistency of 0.7 %. 2 l of 0.7 % pulp was taken into a vessel (Ø 160 mm). The vessel was placed under the Netzsch ShearMaster mixer and clamped in. A mixing plate (Ø 83 mm) was placed at the bottom of the vessel. The pulp was mixed at 500 rpm and then diluted with tap water to a volume of 8 l, so that the final consistency was 0.18 %.

Otherwise, the forming operation and subsequent couching followed the same procedures as in the case of foam forming. In particular, the vacuum was applied for a similar period (about 10 s) as in the case of foam forming.

Adjusting solids content before pressing

After forming, the foam-formed sheets had much higher solids content (16.9 %) than the water-formed sheets (7.5 %). This difference was caused by the higher consistency and the lower surface tension of water in foam forming together with high permeability of the foam-formed fibre networks (Koponen et al. 2017) and their uniform dewatering (see Results and Discussion).

In order to make the compression measurements comparable, the solids content was adjusted to 20 % for both types of sheets by free air drying at room temperature before pressing. This was done by placing a sample inside a draftshield with its door almost closed and stabilizing the moisture content over several minutes before testing. As water transport in wet paper is quite fast, any significant gradient in the moisture content was probably avoided by this approach. After the solids content adjustment, the handling of the samples was easier in the wet pressing experiments.

Measuring thickness with the Lloyd instrument

The Lloyd LR10K material testing device was used to measure the thickness of wet sheets right after forming, before pressing (at 20 % solids content) and after pressing.

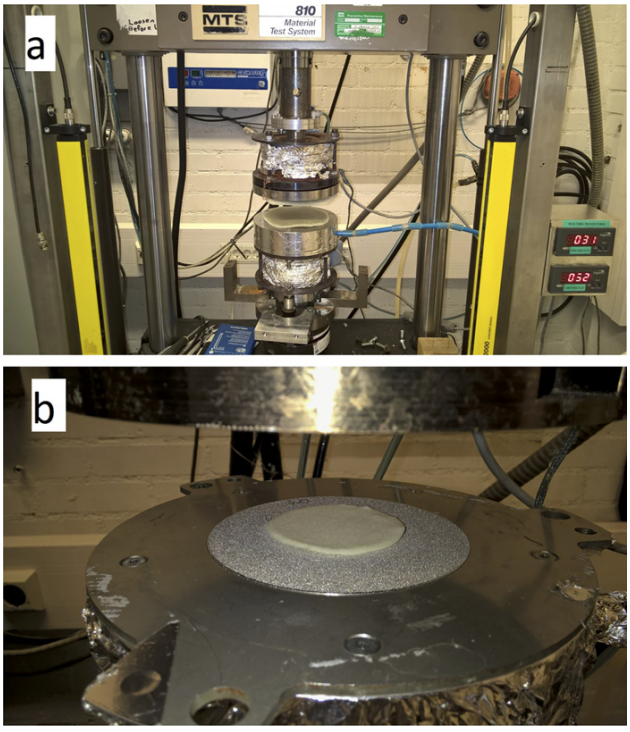

Figure 1: a) MTS pressing device. b) The smooth top and sintered bottom pressing plates together with a wet paper sample. No felts were used in the current study.

A wet sheet was covered with plastic sheets during the measurement, so that the moisture content remained unaffected. The sample was placed between two compression heads (Ø 30 mm). By measuring the distance of the heads at the very small pressure of 1.4 kPa, the sample thickness could be recorded without changing the sheet structure. The initial thickness immediately after water forming was 2.54±0.07 mm and after foam forming 1.95±0.02 mm. This difference was caused by the large 9 %-unit deviation in the moisture contents. At the equal 20 % moisture content, the thicknesses were closer to one another, 2.14±0.09 mm (water) and 1.92±0.07 mm (foam).

Wet pressing with an MTS device

A modified MTS device (Hii et al. 2012) was used to press the wet sheets and simultaneously follow their compression behaviour. The device applied a high pressure pulse between heated top and bottom plates, see Figure 1. The force and position data was recorded at a 0.1 ms interval. The small deformation of the MTS device mechanics under high pressure was deducted from the position data to obtain the true thickness development of a wet sample. This was done by first calibrating the position against a varied static load and then subtracting the remaining device compression obtained with dynamic pressure pulse for an incompressible plastic test sample. In order to help the interpretation of results, no felts were used in this study. Instead, the wet samples were placed between a smooth metallic top plate and a sintered bottom plate, so that water was removed through the sintered plate during pressing. Both the top and bottom plates were heated to a temperature of 45 °C. Samples with a diameter of 53 mm were cut from the wet sheets for the pressing experiments. The peak pressure was adjusted to 6.0–8.5 MPa in all measurements. The pressing time varied in the range of 20–1000 ms. The shortest pulses corresponded to current roll-type (board machines) and shoe-type (high-speed paper machines) presses. On the other hand, the very long pulses were applied to test a case with no limitation to dewatering time. Possible new pressing technologies could be found in between these two extremes. At least three parallel measurements were carried out for each experimental case. The pressed samples were stored in vapor-sealed boxes for later thickness measurements. A few of the samples were also dried with standard methods.

Layered fibre orientation analysis

The orientation of fibres in different layers of the formed fibre network was analysed for dried samples after wet pressing. A sample was split into 18 layers by a laminating technique, and the layers of the size 72 mm × 72 mm were imaged by a desktop scanner. The magnitude and direction of the gradient vectors were determined from every image element. Parameters such as orientation anisotropy and orientation angle could be determined from the elliptic shape of the distribution pattern with axes a and b. The anisotropy $e = 1-b/a$ describes the intensity of orientation ranging from 0 (isotropic) to 1 (complete orientation with all fibres aligning in the direction of foam/suspension flow during forming). This laboured analysis was carried out for one sample only for both forming methods.

Estimation of volume fractions

The interpretation of results is supported by simple calculations of the volume fractions of fibres, water and air based on the measured sheet thickness and the solids content. The total sheet volume V_T is devided into the volumes of fibres (V_f), water (V_w) and air (V_{air}):

$$V_T = V_f + V_w + V_{air}. \quad (1)$$

The fibre (excluding lumen and wall porosity) volume fraction can be expressed in terms of fibre-wall density ρ_f (=1500 kg/m^3 (Niskanen 2008)), grammage g and sheet thickness h:

$$\frac{V_f}{V_T} = \frac{M_f/\rho_f}{A\,h} = \frac{g}{\rho_f h}. \quad (2)$$

Here M_f is the dry fibre mass and A is the sheet area. Similarly, the water (mass M_w) volume fraction in terms of solids content $sc = 100M_f/(M_f + M_w)$ reads as

$$\frac{V_w}{V_T} = \frac{M_w/\rho_w}{A\,h} = \frac{g(100 - sc)}{\rho_w h\, sc}, \quad (3)$$

where ρ_w (=1000 kg/m^3) is the density of water. Equations (1–3) lead then to an equation for the volume fraction of air,

$$\frac{V_{air}}{V_T} = 1 - \frac{g}{h}\left(\frac{1}{\rho_f} + \frac{100 - sc}{\rho_w\, sc}\right). \quad (4)$$

Results and discussion

Fibre network structure

The fibre network structure was analysed after wet pressing and drying, when the sheet density (for 50 ms pressing pulse) was 137 kg/m^3 for foam forming and 166 kg/m^3 for water forming. The sheets had relatively low thickness (1.46 mm for foam, 1.20 mm for water) compared to the average fibre length 2.2 mm. For geometric reasons, the fibre orientation could be expected to be in-plane for both forming methods with very few fibre segments oriented towards thickness direction. In fact, this has been shown earlier by Hjelt et al. 2011 for similar pulp using X-ray tomography imaging. However, the layered fibre orientation analysis revealed differences in the lateral orientation for the two forming methods, see Figure 2. The average orientation anisotropy of the foam-formed sheet was slightly higher, 0.54 (corresponding to the "MD/CD" ratio 2.2), than the value 0.39 (ratio 1.7) of the water-formed sheet. Moreover, the surfaces of the foam-formed sample had higher orientation anisotropy than the middle part (see Figure 2a), where the anisotropy was similar or even lower than in the water-formed sample. The local orientation anisotropy varied quite little over the water-formed sample (Figure 2b).

The strong surface orientation of fibres in foam forming comes probably from sliding bubble layers under shear flow (Tcholakova et al. 2008) whereas inside the foam, a tumbling instability prevent the fibres to be aligned with the flow (Langlois and Hutzler 2017) leading to the peculiar fibre orientation distribution of Figure 2a.

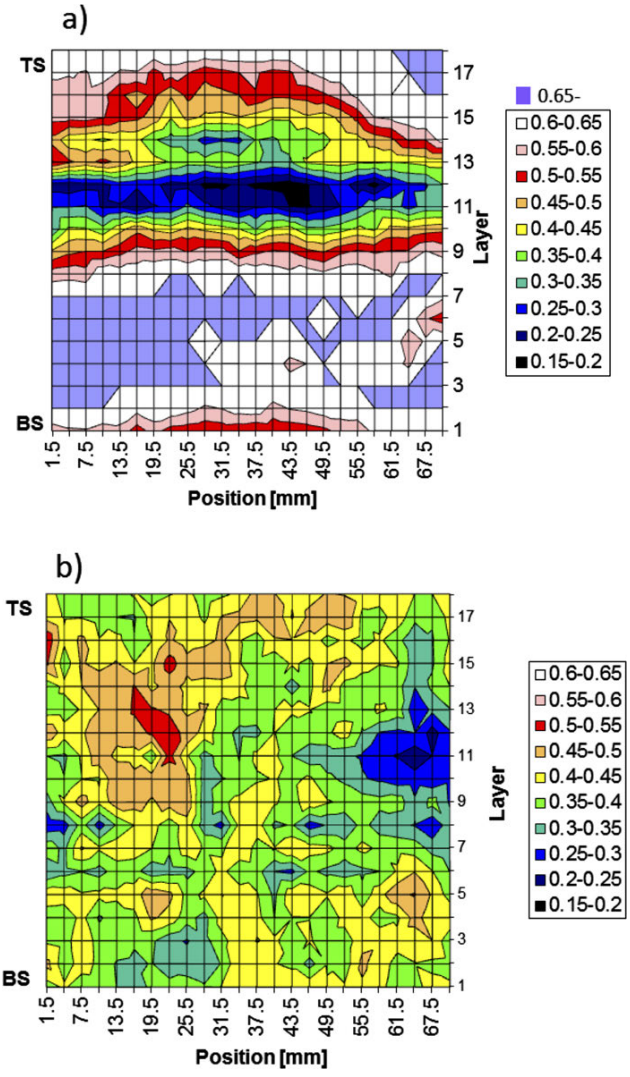

Figure 2: Fibre orientation anisotropy in different layers of a) foam-formed and b) water-formed samples. TS refers to the top side and BS to the bottom (wire) side. The various anisotropy levels (averaged over one direction of a square sample) are shown by different colours.

Another important difference was the excellent formation of the foam-formed sheets. The poorer formation of the water-formed sheets was seen both visually and by measuring the optical formation. The specific formation index (square root of the standard deviation of the gray level) was 6.4±0.2 for water-formed and 4.7±0.1 for foam-formed dried sheets calculated from an area of 74 mm × 59 mm. The formation improvement for foam forming has been seen in earlier works as well (Smith and Punton 1975, Lehmonen et al. 2013).

Pressing single sheet vs. layered structure

The experimental setup and interpretation of the position data was first checked by comparing the compression behaviour of one sheet with that found for a pile of three sheets. The experiment was carried out at equal 20 % solids content in both cases. The total pressing time was 50–110 ms, and the peak pressing force was 6–8 MPa. Having a clearly higher grammage and thickness for the 3-ply structure allowed us to confirm that the sintered plate was able to remove the compressed water fast enough. Moreover, the comparison of the two types of structures allowed us to make sure that the position measurement data was interpreted correctly. A wet sample began to lose its thickness immediately after the force sensor recorded a finite value. This moment was followed carefully in all experiments.

Figure 3 shows the applied pulses and the resulting average thickness developments during pressing for the two types of structures and forming methods. In Figure 3, all curves begin at the moment (time 0) when a finite force value was recorded. This happened earlier for the foam-formed samples, which caused a shift in the location of the main peak as compared to the corresponding water-formed samples. A rapid initial compression (relative change of thickness) of the unpressed sample was already seen at a very small pressure (below 50 kPa), and roughly half of the final compression was already achieved below 250 kPa pressure. At any given pressure level, the 3-ply structure led to a relatively smaller compression than the corresponding single sheet (see Figure 3c). According to Darcy's law (Niskanen 2008), the capillary penetration rate is directly proportional to the pressure gradient, which is inversely proportional to the sample thickness. Thus, water removal is expected to be slower from the thick 3-ply structure, leading to longer sustaining hydraulic forces, which slightly reduce the compression rate as well. Refering to the pressing theory (McDonald and Kerekes 2017), an increase in basis weight, here from 1-ply to 3-ply structure, leads to a more flow controlled (limited) situation with less water removal and compression at a given press impulse. This seems to be the case for both forming methods in Figure 3c, even though the flow control is stronger in the case of water forming.

The foam-formed sample was compressed faster than the corresponding water-formed sample. This qualitative difference in the compression behaviour for the two forming methods did not depend on grammage (1 vs. 3 sheets). Despite 10–15 %-units larger total compression (Figure 4a), the recovered thickness after removing the

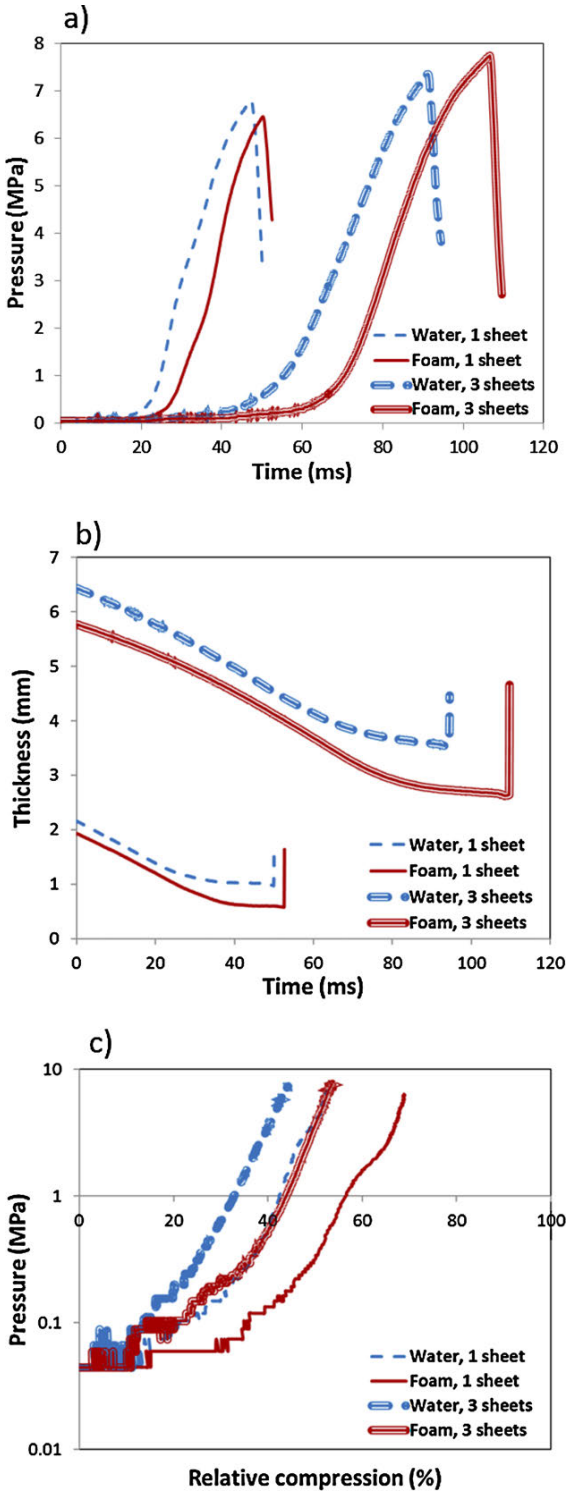

Figure 3: a) The applied pressing pulses on wet foam and water formed single-sheet and 3-ply structures. After reaching the maximum value, the pressure drops rapidly to zero, which is only partly shown in the plot. b) The thickness development during pressing. The final value was obtained by a separate measurement of the sample thickness after the pressing. c) Relative compression of the samples for varied pressure. The solids curves correspond to foam forming and the dashed curves to water forming. The tests on a 3-ply structure correspond to the thicker curves.

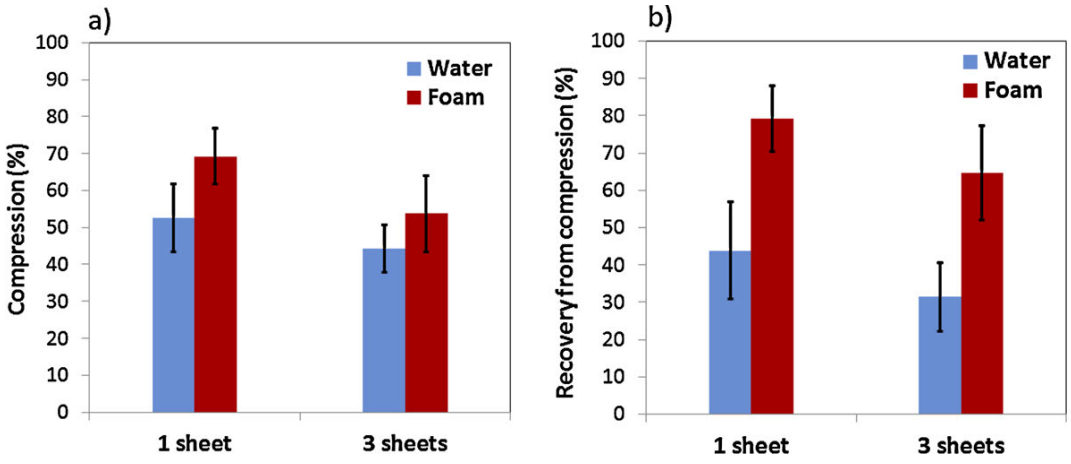

Figure 4: a) Average compression during pressing was higher for the foam-formed (red bars) fibre network than the water-formed network (blue bars). b) Foam forming led to better average thickness recovery after pressing than water forming. The error bars show the standard deviation.

pressing load as compared to the initial unpressed sample thickness was about 30 %-units higher for the foam-formed sheets than the water-formed sheets, see Figure 4b. This led to a better final bulk for the foam-formed sheets even when the water-formed sheets had an initially higher bulk because of their low solids content after forming. The bulk improvement obtained with foam forming was particularly striking as the compression experiment was carried out after adjusting the solids content to the same 20 % level before the pressing.

Figure 5 shows the changes in solids content together with the thickness per sheet. These results did not significantly depend on whether they were measured using one sheet only or with a 3-ply structure. In other words, neither the total compression nor the final water removal were sensitive to the grammage. According to Figure 5, in addition to bulk, solids content after pressing was also significantly higher for foam forming than for water forming even though the initial level was equalized to 20 %.

The data shown in Figure 5 allows one to estimate the changes in air and water fractions caused by the pressing, see Table 1. Immediately after forming, there is already a significant proportion (43 %) of air in the foam-formed sheets, whereas free water fills the pores of water-formed sheets completely (air fraction essentially vanishes). After stabilising the solids content to 20 %, both types of sheets have already roughly a half of the volume filled with air. Moreover, the water fraction (water mass relative to dry fibre mass) is equal to 4.0 in both cases. Because of the relatively long 50–110 ms pulse, the final volume fractions after pressing (Table 1) are very similar for one sheet and a 3-ply structure even though initial water removal and compression (Figure 3c) rates slightly differ for these cases. The final mass water fraction is slightly lower for foam (1.5) than for water forming (1.7). Roughly half of the remaining water (19 % of the total volume for foam forming and 22–23 % for water forming) is bound to fibres.

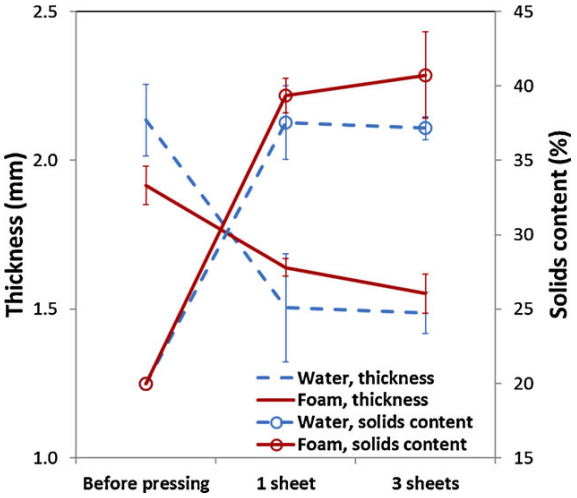

Figure 5: Average thickness and solids content (open circles) before and after pressing for foam (solid curve) and water forming (dashed curve). Single-sheet thickness is shown also for the case of having three sheets together during pressing. The solids content was adjusted by free air drying to an equal 20 % level before the pressing. The bars show the standard deviation.

The above differences in the dewatering behaviour and compression recovery for foam and water formed sheets are probably related to the differences in their fibre network structures. The poorer formation in water forming discussed earlier may cause a larger local permeability

Table 1: Volume fractions of fibres, water and air estimated using Equations 2–4 for the various studied cases. The last column gives the estimated mass of water relative to the dry fibre mass.

		Thickness (mm)	Solids content (%)	ESTIMATED VOLUME FRACTIONS			Mw/Mf
				Air	Water	Fibres	
AFTER FORMING							
	foam	1.95	16.9	0.43	0.50	0.07	4.9
	water	2.54	7.5	-0.02	0.97	0.05	12.3
AT 20 % SOLIDS							
	foam	1.92	20.0	0.51	0.42	0.07	4.0
	water	2.14	20.0	0.56	0.37	0.06	4.0
AFTER PRESSING							
50–110 ms pulse							
	foam, 1 sheet	1.64	39.4	0.73	0.19	0.08	1.5
	water, 1 sheet	1.50	37.5	0.69	0.22	0.09	1.7
	foam, 3 sheets	1.55	40.7	0.73	0.19	0.09	1.5
	water, 3 sheets	1.49	37.2	0.68	0.23	0.09	1.7
20 ms pulse sequence							
1st	foam	1.64	36.7	0.71	0.21	0.08	1.7
	water	1.39	33.7	0.62	0.28	0.10	2.0
2nd	foam	1.39	45.8	0.73	0.17	0.10	1.2
	water	1.25	43.6	0.69	0.21	0.11	1.3
3rd	foam	1.28	49.3	0.74	0.16	0.10	1.0
	water	1.24	46.6	0.71	0.19	0.11	1.1
1000 ms pulse							
	foam	1.01	53.0	0.69	0.18	0.13	0.9
	water	0.95	48.4	0.63	0.23	0.14	1.1

variation and thus a less uniform dewatering in this case. Moreover, the average permeability of the foam-formed fibre network structure is significantly higher than for the water-formed network (Koponen et al. 2017) because of a significant proportion of relatively big pores (Kinnunen et al. 2013, Al-Qararah et al. 2015). Moreover, the surface tension of water is smaller in foam forming because of the added surfactant. The improved dewatering leads to a higher solids content of the foam-formed sheets after pressing.

On the other hand, the excellent formation of the foam-formed sheets leads to a more uniform distribution of compressive stresses. The inelastic creep deformations during compression are exponentially proportional to the stress (Brezinski 1956, Habeger and Coffin 2000, Ketoja et al. 2007). The peak stresses and subsequent plastic network deformations (Vomhoff 1998) are therefore expected to be lower for the foam-formed fibre network than the water-formed network. Thus, the recoverable part of the compressive strain (i. e. elastic strain and creep recovery) is larger for the foam-formed sheets. This underlies the thickness behavior of Figure 3b. The fibre orientation differs for the two forming methods as well (refer to Figure 2), but the orientation is not expected to affect inelastic or recovered deformations to a similar extent.

Effect of pressing pulse duration

In addition to varied structural thickness, we also tested the effect of the duration of a single pressing pulse on the compression behaviour. In addition to a short 20 ms pulse, a very long pressing of 1000 ms was tried as well, as shown in Figure 6. In other words, a typical short pulse of roll or shoe type presses was compared with the pulse (much longer than a pulse of an industrial nip) without flow time limitation. The applied pulse form was very similar for both forming methods, see Figure 6a. The peak pressure was 7.7 MPa for the short pulse and 7.3–7.4 MPa for the long one. Three parallel long-pulse tests were highly reproducible, and their average result is shown in Figure 6. For the short pulse, the scatter between parallel measurement was larger for both types of sheets. Thus, the average of seven parallel measurements are shown in this case.

Foam and water formed sheets differed clearly for both pulse types. The slightly larger compression of the foam-formed sheet was generally compensated for by the clearly better thickness recovery after the pressing load was removed (Figure 6b). Somewhat counter-intuitively, the long pulse led not only to a lower final thickness but also to a smaller relative compression (for water forming) and recovery (for both forming methods). The complexity of

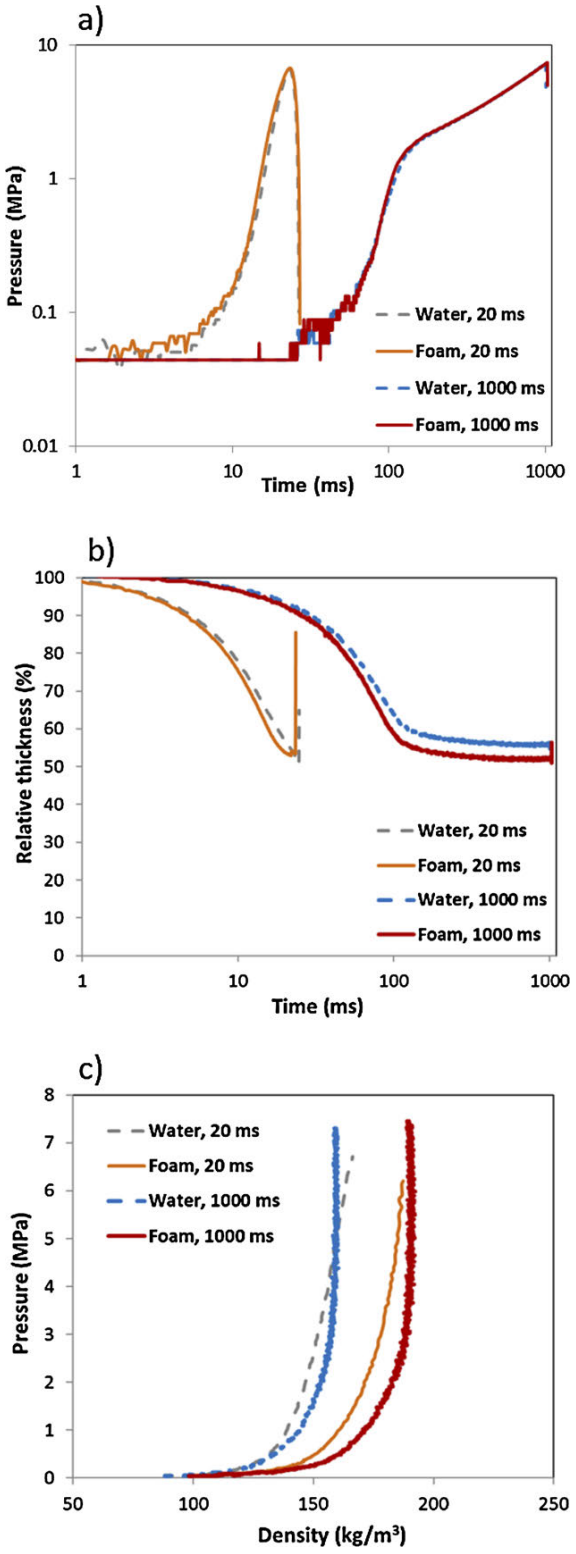

Figure 6: a) Varied pressing pulses applied on wet foam and water formed sheets. b) The development of relative thickness during pressing. The final value was obtained by a separate measurement of the sample thickness after the pressing. c) The development of fibre network density (water excluded) during pressing.

the compression dynamics is shown by the exponential density-pressure curves of Figure 6c. For a very low pressure below 0.2 MPa, the density development is similar for both types of pulses. At intermediate pressures, the rapid short pulse is associated with a larger hydraulic force because of finite permeability. In other words, the pressing in this region is flow controlled, and the hydraulic force carries a part of the total load. Therefore, the fibre-network density stays below that of the long pulse for an equal total pressure. Near the peak pressure, the load is carried out mainly by the fibre network (Carlsson et al. 1983). The resulting deformations are expected to be the smaller for the long pulse because of the higher solids content (the final solids content is 53 % for foam and 48 % for water forming) improving fibre network stiffness. This causes the approach and even crossing of density curves in Figure 6c near the peak pressure. On the other hand, significant plastic deformations take place earlier during the long pulse with higher press impulse, which diminishes the thickness recovery after pressing.

The rise of the pressure at lower densities for water forming results from the non-uniform in-plane material distribution in the sheets. The high-density (or thick) regions take up a major load, and they cause the local pressure to increase relatively early during compression. The stress distribution becomes uneven limiting the recovery as well. The foam-formed sheets distribute the stress more evenly, which allows both high compression and recovery. Thus, the density difference between foam and water forming does not depend on whether the pressing is flow or pressure limited.

Using the long pulse, the final water fraction becomes almost a half of that achieved with the short pulse (see Table 1), leading to a larger proportion of the fibre volume in the pressed sheet. The estimated values of the water fraction, 0.9 for foam forming and 1.1 for water forming, are slightly higher than a typical fibre saturation point of mechanical fibres, 0.5–0.7 (Niskanen 2008).

Three consecutive pressing pulses

The industrial wet pressing operation usually consists of several subsequent short pulses. We studied this operation by pressing the sheets three times consecutively. The duration of a pulse was around 20 ms. In the case of foam-formed sheets, the average peak pressure was 7.3–7.4 MPa for all pulses. For water-formed sheets, the peak pressure varied from 6.9 MPa (1st pressing) to 8.4 MPa (2nd pressing), which affected the compression behavior as well. There

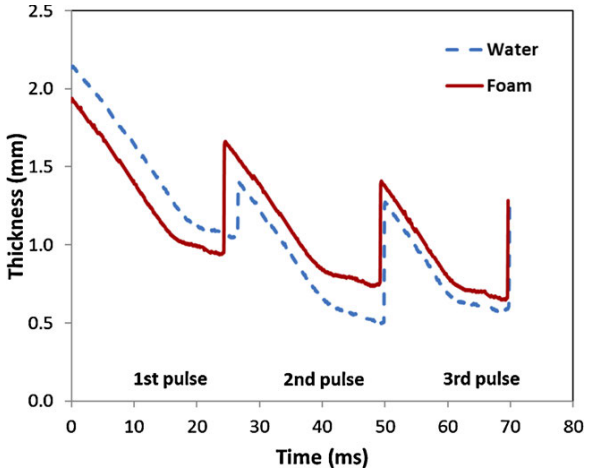

Figure 7: Thickness development during the sequence of three subsequent pressing pulses for foam (solid curve) and water forming (dashed curve). In the experiment, the pulses were separated by a significant time interval, which is not shown in the figure.

was a significant delay (a couple of hours) between subsequent pulses. Thus, the experiment did not fully mimic the fast online process dynamics. However, the findings can be used to estimate how well the differences in the behaviour of foam and water formed sheets are preserved when the number of pulses is increased.

Figure 7 shows the observed thickness changes during (and after) the pulses for both forming methods. A major part of the reduced thickness during a pulse springs back after the pulse has ended. As seen in Figure 8, the relative compression has quite a similar level for both forming methods and for all pulses. The larger compression of the water-formed sheets for the 2nd pulse results from the higher peak pressure in this case. However, the recovery from compression (spring back of thickness) was significantly different between foam (70 %) and water (28 %) forming after the first pulse (Figure 8b). Interestingly, for the second and third pulses, the water-formed sheet recovered slightly better from compression than the foam-formed sheet. After the third pulse, the recovery was almost 100 % for the water-formed sheet, whereas for the foam-formed sheet, the recovery was not as complete, i. e. approximately 85 %.

Figure 9 summarizes the changes in thickness and solids content after the pulses. Solids content was adjusted to 20 % in both types of sheets before pressing. The thickness before pressing was higher for water-formed sheets than for foam-formed sheets. After the first pulse, the situation was already the opposite, and the later pulses did not change the order any longer. However, after the last pulse, the thicknesses for the two forming methods were already almost equal. On the other hand, the solids content became higher with foam than water forming after the first pulse, and this difference stayed at the same level throughout the pulse sequence.

According to these results, the different sheet structures for foam and water forming have strong effects for the first pulse, when mainly inter-fibre water is removed from a sheet. However, after this pulse, when solids content is already above 30 %, water is mainly compressed from the fibre walls and lumens (Hii et al. 2012), so that the variations in the network structures play a minor role. This is reflected in Table 1, where all volume fractions change rather little for the 2nd and especially for the 3rd pulse. This explains the quite similar compression and dewatering behaviours observed for foam and water forming for

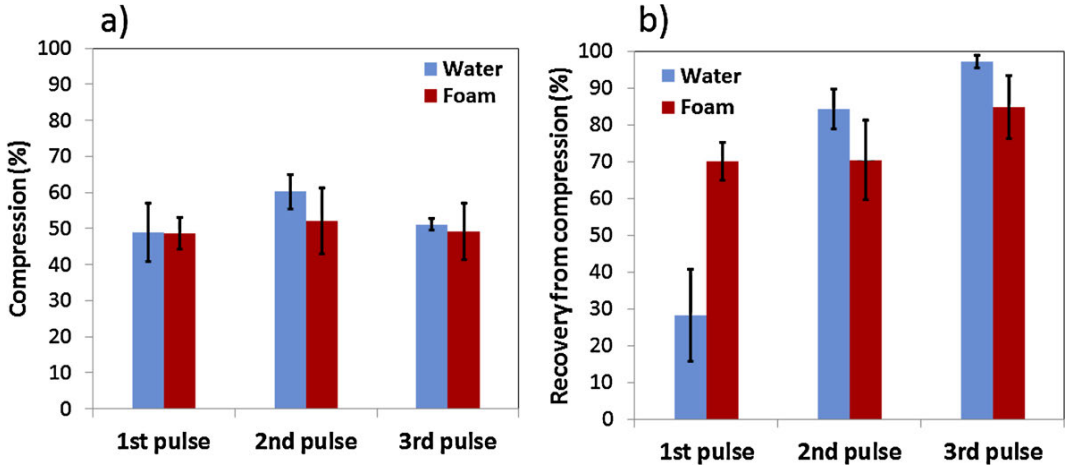

Figure 8: Relative compression (a) and thickness recovery (b) for three subsequent pressing pulses for water (blue bars) and foam forming (red bars). The error bars show the standard deviation.

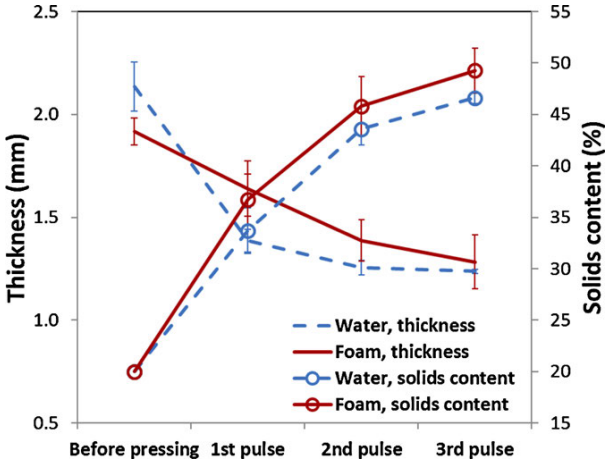

Figure 9: The development of sheet thickness and solids content with an increasing number of pressing pulses for foam and water forming. The solids curves correspond to foam forming and the dashed curves to water forming. The measured values of solid contents are indicated by open circles. The bars show the standard deviation.

these latter pulses. The solids content of the foam-formed sheets increases with the 2nd pulse but the air proportion is not much affected, which indicates that the water is removed mainly from fibre walls. With increasing number of pulses, the air content in water-formed sheets approaches that of the corresponding foam-formed sheets as water is removed mainly from fibres only. The water fractions after the 3rd short pulse are already close to those obtained for the very long 1000 ms pulse. Moreover, the changes in relative fibre and air volumes saturate as the recovery from compression is almost complete according to Figure 8b.

Conclusions

Foam and water formed wet sheets behave quite differently in laboratory wet pressing experiments. Despite larger relative compression, the foam-formed sheets recover their thickness better than the water-formed sheets leading to higher bulk after the load is removed. This is probably related to the excellent formation obtained with foam forming, which helps in reducing peak stresses that drive plastic deformations during compression. The bulk advantage is gradually reduced when the number of pressing pulses is increased. Moreover, the dewatering is also more effective for the foam-formed sheets because of their higher permeability and lower water surface tension. This should be taken into account in defining pressing strategies. In particular, excessive consecutive pressing of the foam-formed web structures should be avoided when the target is to reach the highest bulk level in the produced web.

Acknowledgements: We would like to thank Ilkka Nurminen for pulp preparation, Päivi Sarja for making the wet sheets, Christian Orassaari for running the MTS device at Aalto University, and Annika Ketola, Merja Selenius and Daniel Koskelo for the help with the measurements. Moreover, helpful discussions with Harri Kiiskinen, Antti Koponen and Jarmo Kouko are greatfully acknowledged.

Funding: This work was partly supported by Academy of Finland (Project "Surface interactions and rheology of aqueous cellulose-based foams").

Conflict of interest: The authors declare no conflicts of interest.

References

Al-Qararah, A. M., Ekman, A., Hjelt, T., Ketoja, J.A., Kiiskinen, H., Koponen, A., Timonen, J. (2015) A unique microstructure of the fibre networks deposited from foam–fibre suspensions. Colloids Surf. A, Physicochem. Eng. Asp. 482:544–553.

Brezinski, J. P. (1956) The creep properties of paper. Tappi J. 39(2):116–128.

Carlsson, G., Lindstrom, T., Norman, B. (1983) Some basic aspects on wet pressing of paper. J. Pulp Pap. Sci. 9(4):101–106.

Habeger, C. C., Coffin, D. W. (2000) The role of stress concentrations in accelerated creep and sorption-induced physical aging. J. Pulp Pap. Sci. 26(4):145–157.

Hii, C., Gregersen, Ø. W., Chinga-Carrasco, G., Eriksen, Ø. (2012) The effect of newsprint furnish composition and sheet structure on wet pressing efficiency. Nord. Pulp Pap. Res. J. 27(4):790–797.

Hjelt, T., Kinnunen, K., Lehmonen, J., Beletski, N., Hellén, E., Liljeström, V., Serimaa, R., Miettinen, A., Kataja, M. (2011) Intriguing structural and strength behavior in foam forming. In: Proc. Progress in Paper Physics Seminar. Graz, p. 135.

Ketoja, J. A., Tanaka, A., Asikainen, J., Lehti, S. T. (2007) Creep of wet paper. In: Proc. International paper physics conference. Gold Coast, Australia. 5 pp.

Kinnunen, K., Lehmonen, J., Beletski, N., Jetsu, P., Hjelt, T. (2013) Benefits of foam forming technology and its application in high MFC addition structures. In: Proc. 15th Pulp and Paper Fundamental Research Symposium, Cambridge.

Koponen, A., Ekman, A., Mattila, K., Al-Qararah, A. M., Timonen, J. (2017) The effect of void structure on the permeability of fibrous networks. Transp. Porous Media 117:247–259.

Langlois, V. J., Hutzler, S. (2017) Dynamics of a flexible fibre in a sheared two-dimensional foam: Numerical simulations. Colloids Surf. A, Physicochem. Eng. Asp. 534:105–111.

Lehmonen, J., Jetsu, P., Kinnunen, K., Hjelt, T. (2013) Potential of foam-laid forming technology in paper applications. Nord. Pulp Pap. Res. J. 28:392–398.

McDonald, J. D., Kerekes, R. (2017) Pragmatic mathematical models of wet pressing in papermaking. BioResources 12(4):9520–9537.

Niskanen, K. ed. Paper Physics, 2nd ed., Paperi ja Puu Oy, Helsinki. 360 pp., 2008.

Pikulik, I. I., McDonald, D., Mentele, C. J., Lange, D. V. (1998) The effect of refining, forming, and pressing on fine paper quality. Tappi J. 81(6):122–130.

Pöhler, T., Jetsu, P., Isomoisio, H. (2016) Benchmarking new wood fibre-based sound absorbing material made with a foam-forming technique. Build. Acoust. 23(3–4):131–143.

Poranen, J., Kiiskinen, H., Salmela, J., Asikainen, J., Keränen, J., Paakkonen, E. (2013) Breakthrough in papermaking resource efficiency with foam forming. In: Proc. TAPPI PaperCon 2013, 1. pp. 807–814.

Radvan, B., Gatward, A. P. J. (1972) The formation of wet-laid webs by a foaming process. Tappi J. 55:748–751.

Smith, M. K., Punton, V. W. (1975) Foam can improve formation. Pulp Pap. Can. 76(1):55–58.

Tcholakova, S., Denkov, N. D., Golemanov, K., Ananthapadmanabhan, K. P., Lips, A. (2008) Theoretical model of viscous friction inside steadily sheared foams and concentrated emulsions. Phys. Rev. E 78:011405.

van Lieshout, M. (2006) The effect of wet pressing on paper quality. Ph. D. thesis. Groningen: University of Groningen. 170 pp.

Vomhoff, H. (1998) Dynamic compressibility of water saturated fibre networks and influence of local stress variations in wet pressing. Ph. D. thesis, Stockholm: Royal Institute of Technology. 68 pp.